Environmental Science & Technology

Article

pubs.acs.org/est

Bringing High-Rate, CO_2-Based Microbial Electrosynthesis Closer to Practical Implementation through Improved Electrode Design and Operating Conditions

Ludovic Jourdin,[*,†,‡,§] Stefano Freguia,[†,‡] Victoria Flexer,[†,∥] and Jurg Keller[†]

[†]Advanced Water Management Centre and [‡]Centre for Microbial Electrochemical Systems, The University of Queensland, Gehrmann Building, Brisbane, QLD 4072, Australia

Supporting Information

ABSTRACT: The enhancement of microbial electrosynthesis (MES) of acetate from CO_2 to performance levels that could potentially support practical implementations of the technology must go through the optimization of key design and operating conditions. We report that higher proton availability drastically increases the acetate production rate, with pH 5.2 found to be optimal, which will likely suppress methanogenic activity without inhibitor addition. Applied cathode potential as low as −1.1 V versus SHE still achieved 99% of electron recovery in the form of acetate at a current density of around −200 A m^{-2}. These current densities are leading to an exceptional acetate production rate of up to 1330 g m^{-2} day^{-1} at pH 6.7. Using highly open macroporous reticulated vitreous carbon electrodes with macropore sizes of about 0.6 mm in diameter was found to be optimal for achieving a good balance between total surface area available for biofilm formation and effective mass transfer between the bulk liquid and the electrode and biofilm surface. Furthermore, we also successfully demonstrated the use of a synthetic biogas mixture as carbon dioxide source, yielding similarly high MES performance as pure CO_2. This would allow this process to be used effectively for both biogas quality improvement and conversion of the available CO_2 to acetate.

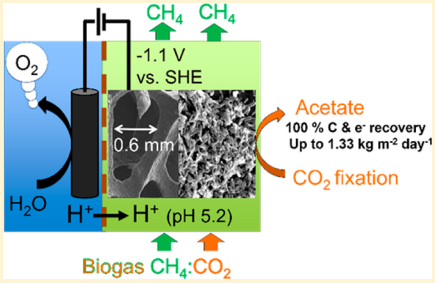

INTRODUCTION

Global concern over CO_2 accumulation in the atmosphere and fossil resource depletion has led to increased research efforts into alternative technologies for the sustainable production of energy and chemicals. Creating novel approaches for the direct transformation of carbon dioxide into valuable end-products is very attractive.[1,2] Consequently, many CO_2-based production processes have been and are being investigated and developed, as recently reviewed by Mikkelsen at al. (2010).[3] Microbial electrosynthesis (MES) from CO_2 is a biocathode-driven process that holds much promise for the production of chemicals.[2,4−6] MES relies on the conversion of electrical energy into valuable extracellular organic molecules by autotrophic electroactive microorganisms.[7] MES can also be envisioned as an interesting option to capture and store harvested intermittent renewable (electrical) energy such as wind and solar energy into stable, high-energy-density liquid or solid products that are easily transportable.[8]

MES is still regarded as a nascent concept, with the first proof of concept of pure acetogenic microorganisms able to derive electrons from solid-state electrodes (as sole energy source) to catalyze the reduction of CO_2 to acetate being described only a few years ago.[9,10] However, since then, an increasing number of articles has been published on this exciting new concept, with significant performance improvements and improved understanding of the underlying mechanisms bringing MES closer to a practically feasible technology.[2,6,11−20] Marshall et al. (2012) first showed the ability of mixed cultures to perform microbial electrosynthesis to acetate, with an improved production rate over long-term operation.[16,17] Initially, only acetate could be produced by MES from CO_2; however, a recent study has showed the simultaneous conversion of CO_2 into a mixture of products composed of acetate, butyrate, ethanol, and butanol.[12] The higher market value and demand of some of these organics (e.g., butanol) compared to acetate makes their direct production from CO_2 very interesting. Nevertheless, high product specificity and production rates are regarded as key parameters that could enable large-scale applicability of such a technology.[21] Recent studies have shown that even mixed cultures can generate a high product yield and specificity.[13] Indeed, enriched mixed microbial consortia were able to convert 100 ± 4% of the electrons derived from an electrode and of the total CO_2 consumed toward one single final extracellular product, acetate,[13] which makes its extraction easier. The electrode used in this work was a highly biocompatible, three-dimensional hierarchical cathode material with surface modifications based on electrophoretic deposition methods that are easily reproducible and scalable (EPD-3D). In addition, very high electron consumption (ca. −102 A m^{-2} cathodic current density) and acetate production rates (ca. 685

Received: September 14, 2015
Revised: December 9, 2015
Accepted: January 26, 2016
Published: January 26, 2016

DOI: 10.1021/acs.est.5b04431
Environ. Sci. Technol. 2016, 50, 1982−1989

± 30 g m^{-2} day^{-1} equivalent to 66 kg m^{-3} day^{-1}) could be achieved, which is similar to that achieved in established industrial fermentation processes.[13] An in-depth analysis of the electron fluxes and mechanisms occurring in this system has also been reported.[14] It demonstrated that the main electron-transfer mechanism from the electrode to the terminal electron acceptor, CO_2, occurs via H_2. The H_2 production was found to be biologically induced, likely through the biological synthesis of metallic copper particles.[14] Long-term operation also showed successful with microorganisms sustaining themselves in such specific MES conditions, in both fed-batch and continuous mode.[2,11,13,17] Lowering the pH from near neutral to 5 was shown not to affect acetate production, while concomitant H_2 production significantly increased.[15] Another study with slightly acidic (ca. 5.8) pH control was shown to improve microbial electrosynthesis either by the direct effect of low pH, by increasing the substrate availability, or both.[11] At those rates and yields, in-depth investigation toward practical implementation of MES technology becomes relevant and paramount.

Moreover, acetate has many potentially viable applications either as a useful end-product by itself or as a platform for further chemical transformations.[21,22] A high acetate titer, in the order of 11 g L^{-1}, was also achieved, which makes it easier for potential downstream processing.[2,17] Agler et al. (2011) reviewed a range of processes for the production of higher value compounds (e.g., alcohols and long-chain fatty acids) from short-chain carboxylates, such as acetate, described as "the carboxylate platform".[21] Short-chain carboxylates, such as acetate, can be further processed by separate postprocessing steps (e.g., chemical, biochemical, electrochemical, and thermochemical steps). Carbonyls, esters, alcohols and alkanes are examples of high-value end-products generated through such reactions, producing directly usable fuels and industrial solvents.[21] Liu et al. (2015) very recently described a new direct solar-powered process for the production of acetate from CO_2 coupled with the biosynthesis of complex organic molecules from acetate, such as *n*-butanol, PHB biopolymer, and isoprenoid compounds using genetically engineered *Escherichia coli* in a separate vessel.[22] Acetate itself is also widely used as carbon substrate for many industrial biological processes, such as denitrification in wastewater treatment plants. In this regard, MES could become an interesting option for onsite acetate production, e.g., using the CO_2 from biogas and electric energy from methane combustion. However, considerable further process development of all these options is required to maximize the production rates and yields and to identify the most valuable utilization of acetate, or other organics, generated by MES.

Further research is, therefore, needed toward reactor upscaling, optimization of operating conditions, and the search for cheap and easily usable carbon dioxide sources. In this study, we investigated the effect of three different EPD-3D electrode pore sizes (2.54, 0.56, and 0.42 mm average pore diameter) on MES performance from CO_2 to acetate and from both intrinsic and engineering performance standpoints. The significant effects of pH and applied potentials on MES performance were also assessed. MES to acetate was also showed successful as a potential biogas upgrading technology (i.e., to decrease its CO_2 fraction) when biogas was used as the sole, cheap, and readily available carbon dioxide source.

MATERIALS AND METHODS

Electrode Preparation. Multiwalled carbon nanotubes (MWCNT) were deposited via electrophoretic deposition, as reported previously,[13] on reticulated vitreous carbon (RVC) of three different pore sizes (10, 45, and 60 pores per inch (ppi)) to generate a hierarchal porous structure, hereafter called EPD-3D, which we used as biocathode electrodes. Briefly, the dispersed negatively charged MWCNT migrate toward the positive RVC electrode due to the electric field being applied to the dispersion. The MWCNT, due to particle coagulation, then formed a coherent deposit on the RVC surface.

Preparation of the EPD-3D electrodes has previously been reported.[13] They were pierced with a 0.5 mm thick titanium wire that acted as current collector. The electrical connection was reinforced using conductive carbon paint applied at least 1 day prior to the use of the electrodes.

BES performance when using structured 3D electrodes is commonly normalized to the maximal projected area of the electrode, which refers to the maximal footprint of the base of the electrode.[2,23] Alternatively, the total (biofilm accessible) surface area of the electrode, as previously defined for MWCNT−RVC electrodes,[2,13] is being used to assess the intrinsic performance of the electrode materials. Projected and total surface areas for each of the electrodes used in this study are summarized in Table S1. The electrodes had a slightly variable thickness of around 10 ± 1 mm.

For the assessment of performance from an engineering perspective (e.g., size of the reactor), current values, CO_2 consumption, and acetate production have also been normalized to the volume of the cathode electrode, taking into account its 3D nature and the total electrode surface available for biofilm development per unit volume. The volume of the electrodes used in this study are shown in Table S1. The consumption and production rates have also been normalized to actual catholyte volume used in this study (250 mL), although the reactors' configuration (e.g., electrode volume/catholyte volume ratio) was far from being optimized. The calculations of projected surface area, total surface area, and volume of the electrode are shown in the Supporting Information.

All electrodes (with the deposited MWCNTs) were pretreated in a N_2 plasma for 20 min before being introduced in the reactors to remove surface contamination and render the surface hydrophilic.[24]

Source of Microorganisms. Planktonic cells from the microbial electrosynthesis systems described by Jourdin et al.[2] were collected, centrifuged, suspended in fresh catholyte, and used as inoculum for the MESs described in this study. Microbial community compositions of both the inoculum and the enriched consortia were previously reported,[14] with *Acetoanaerobium*, *Hydrogenophaga*, *Methanobrevibacter*, and one New Reference_OTU closely related to *Acetoanaerobium noterae* being found dominant in the enriched community. No soluble organics were therefore introduced in the new reactors. The enriched inoculum was added to a final concentration of about 200 mg_{COD} L^{-1} in each reactor.

Electrochemical Experiments. The reactor design, materials, experimental conditions, medium composition and analytical methods were identical to those described in Jourdin et al.[2,13] and are also presented in the Supporting Information. A total of four microbial electrosynthesis reactors (two of them equipped with one 45 ppi electrode each, one with a 60 ppi

DOI: 10.1021/acs.est.5b04431
Environ. Sci. Technol. 2016, 50, 1982−1989

electrode, and the fourth reactor with two 10 ppi electrodes (as duplicates for current consumption)) were each filled with 250 mL of inorganic medium containing bicarbonate as sole carbon source and polarized at −0.85 V versus SHE for 63−70 days. Final concentration of 1 to 4 g L^{-1} $NaHCO_3$ was added periodically as the sole carbon source. Experiments were carried out under strict anaerobic and dark conditions at 35 °C. The BESs were operated in fed-batch mode. Magnetic bars of same geometrical dimensions and a magnetic stirring rate of 150 rpm were used on each reactor. To suppress methanogenic activity, we added 15 mM 2-bromoethanesulfonic acid. During the experiment, the catholyte medium pH was regularly adjusted to 6.7 by dosing with 1 M HCl as needed. The anolyte contained 6 g L^{-1} Na_2HPO_4 and 3 g L^{-1} KH_2PO_4, and platinum wire was used as the counter-electrode (purity 99.95%, 0.50 mm diameter × 50 mm long, Advent Research Materials, Oxford, England).

Analytical Methods. The concentrations of volatile fatty acids in the liquid phase were determined by a gas chromatography method,[6] and bicarbonate consumption was followed by a total organic carbon analyzer method.[6]

Electrochemical Titration and Off-Gas Analysis Test. The titration and off-gas analysis (TOGA) sensor was first developed by Gapes et al.[25] and Pratt et al.[26] for the study of biological processes in wastewater treatment systems. The TOGA sensor has recently been modified and used in this study as described by Jourdin et al.[14] for its use in combination with bioelectrochemical systems and in microbial electrosynthesis biocathode systems in particular. In this condition, the TOGA sensor allows the continuous monitoring of flow rates of targeted gases (H_2, CH_4, and CO_2) throughout an electrochemical test. A description and schematic of the setup used with the TOGA sensor can be found in the Schematic S1.

The flow rates of the targeted gases were calculated by mass balance using an inert internal standard, argon, which was added to the carrier gas. The flow-rates of H_2 were then converted from mL min^{-1} to mol min^{-1} using the ideal gas law and further converted into mA (i.e., electron flow in the form of H_2) using Faraday's law, which is the representation of H_2 flow plotted and referred to in the Results and Discussion section.

Linear-sweep voltammetry (LSV) experiments from 0 to −1.1 V versus SHE (unidirectional) at a scan rate of 0.1 mV s^{-1} and pH 6.7 in the presence of CO_2 were performed using the TOGA sensor to investigate the effect of applied potential on MES performance. Chronoamperometry tests at −0.85 V versus SHE while screening pH from 6.7 to 3 using the TOGA sensor were also performed to assess the effect of pH on MES performance. A multichannel potentiostat (VMP-3, Bio-Logic SAS, France) was used for all experiments.

Finally, chronoamperometry tests at −0.85 V versus SHE applied cathode potential at pH 6.7 using biogas-like gas mixture (CH_4:CO_2 70%:30% v/v, BOC, Australia) as sole carbon source were performed with the TOGA sensor. This experiment was performed on the MES reactor described in one of our previous studies,[14] on 45 ppi EPD-3D, after the current had decreased to about −30−35 A m^{-2}, possibly due to a large number of LSV experiments conducted on this reactor that may have affected the performance of this biocathode (see details in Figure S1). Without using the TOGA sensor but using the same reactor setup described in this section, the biogas mixture was sparged in the recirculation bottle at a flow rate of 35 mL min^{-1} for about 13 days, and the current and VFA production were followed while a cathode potential of −0.85 V versus SHE was applied at pH 6.7. Chronoamperometry tests using the TOGA sensor were carried out on days 4 and 7, as described above. Soluble CO_2/HCO_3^- was still present in excess in these conditions (biogas sparging and non-optimized reactor). Consequently, changes in CO_2 concentration in the off gas was not detectable; nor was the change in methane concentration.

RESULTS AND DISCUSSION

Mass-Transfer Limitation versus Total Surface Area Per Volume Unit: Effect of 3D Electrodes' Porosity. Starting right after inoculation (day 0), current consumption, carbon dioxide consumption, and volatile fatty acids production were followed for each reactor during days 63 to 70. Results for the three different electrode porosities were compared to assess the respective performances in terms of intrinsic performance as biocathode material and of the engineering upscaling potential. To do so, we normalized results either by total surface area or projected surface area of the electrodes, respectively; the method of normalization is extensively discussed previously.[2,13] For the tests on the 45 ppi electrode, the average of the two duplicate reactors is plotted in Figures 1 and 2 and referred to in the text for each parameter studied. Similarly, the electron consumption average of the two 10 ppi electrodes is plotted and referred to in the text. Results of duplicates were in good agreement and the standard deviation minimal, as seen in Figure 1.

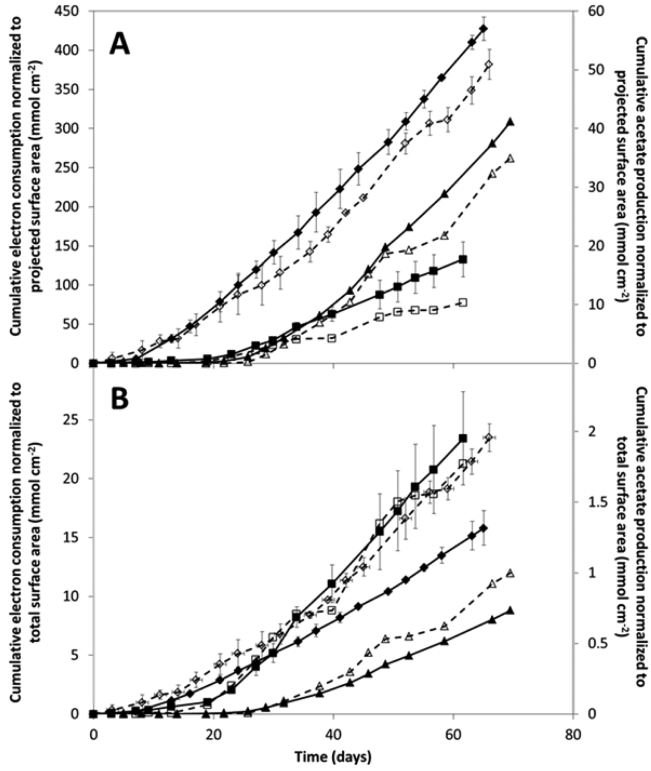

Figure 1. Cumulative electron consumption (full marker) and acetate production (empty marker) over time on 10 ppi (square), 45 ppi (diamond), and 60 ppi (triangle) EPD-3D electrodes, normalized to both projected surface area (A) and total surface area (B).

The cumulative electron consumption and acetate production over time, at constant applied potential of −0.85 V vs SHE, are shown in Figure 1 normalized to both projected (A) and

DOI: 10.1021/acs.est.5b04431
Environ. Sci. Technol. 2016, 50, 1982−1989

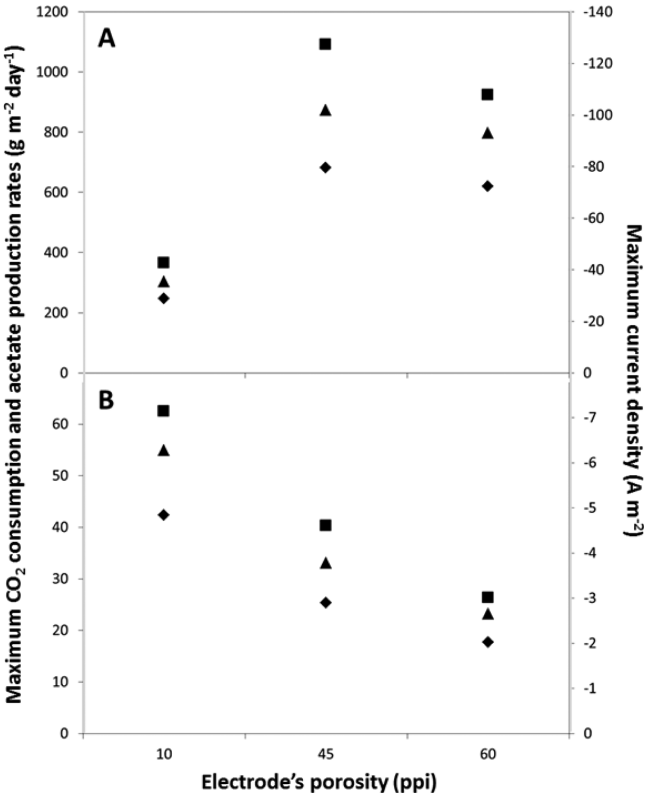

Figure 2. Maximum carbon dioxide consumption rate (square), acetate production rate (diamond), and cathodic current density (triangle) obtained on 10, 45, and 60 ppi EPD-3D, both normalized to projected surface area (A) and total surface area (B).

total (B) surface area. No other volatile fatty acids or alcohols accumulated in any of the reactors, nor was hydrogen detected in the headspace. The transfer of an enriched microbial culture achieved a rapid colonization and activity in all reactors, which is an important demonstration for a successful start-up strategy for larger-scale reactors. The first significant observation is the difference in the start-up time required for each electrode type. On 45 ppi electrodes, current and acetate production started increasing after few days (ca. 3−4 days), while it took about 10 days on the 10 ppi electrodes and even longer (ca. 20 days) on the 60 ppi electrode. It is speculated that the 45 ppi electrode may have an optimal combination of high total surface area and accessibility, which provides a good initial distribution and adhesion of the micro-organisms throughout the electrode.

As previously reported,[2,13] after a first phase of slow electron consumption (start-up phase), electron consumption gradually increased up to a maximum from about 50 days onward for each electrode type (Figure 1A). A similar trend can be observed for the acetate production in each reactor (Figure 1B). Maximal current density (as A m^{-2}) and acetate production rate (as g m^{-2} day^{-1}) were deducted from Figure 1, from the last 15−20 days of the experiment (where rates were steady and maximal), for each electrode type and are shown in Figure 2. Carbon dioxide consumption was also followed over time (not shown), and maximal rates are plotted in Figure 2 as well. Rates normalized by the volume of the electrode (relevant from an engineering perspective as well, e.g., reactor sizing) as well as the actual catholyte volume (250 mL) are also presented in Figure S2. Remarkably, particularly for a mixed culture system, both carbon dioxide and electron conversion efficiencies into acetate were very high and consistent for all three electrode types, with an average of 98 ± 4% and 100 ± 1%, respectively. As discussed in the Introduction section, high product specificity is of critical importance for large-scale implementation of a production technology. Product separation and recovery is one of the main costs of established chemical production plants, such as industrial fermentation.[21,27] Therefore, obtaining one "pure" product instead of a mixture of different products could be a significant benefit for practical applicability of microbial electrosynthesis technology from both a technical and economic point of view. Once again, those electron recoveries were calculated from the last 15−20 days of experiments in which MES performance was maximal on each electrode type. When calculated over the whole period from inoculation, still-high electron recoveries into acetate of 99% and 90% were measured on 45 and 60 ppi electrodes, respectively, whereas only 60% of the electrons were recovered into acetate on a 10 ppi electrode. This may be explained by more extensive biomass growth in the initial stage of the experiment or possibly by the loss of hydrogen when the biofilm was not fully developed (initial phase) due to larger macropore diameter when compared to the other type of electrodes. As explained above, larger macropore diameter may not provide a good initial distribution and adhesion of the micro-organisms throughout the electrode.

Figure 2B shows the efficiency of the process in relation to each electrode's porosity by normalizing the maximum CO_2 consumption and acetate production rates and current density to total surface area. It is clearly evident that the intrinsic performance decreases as the pore diameter decreases, from ca. 42 g m^{-2} day^{-1} of acetate (ca. −6.28 A m^{-2}) for pores with ca. 2.54 mm diameter, to about 2.3 times lower rates when the pores are 6 times smaller (ca. 0.42 mm) (i.e., ca. 18 g m^{-2} day^{-1} of acetate (ca. −2.7 A m^{-2})). This shows that mass transfer of substrate and nutrients or of product to and from the surface of the electrode becomes limiting as the pores within the 3D structured electrode material become smaller. It has to be pointed out that the mixing rate in each reactor was identical (i.e., same size and rotation rate of magnetic stirrer bars) to allow a valid comparison. It is assumed that the mass transfer through the 3D macrostructure itself (i.e., in the liquid phase) is the limiting factor rather than the mass transfer within the biofilm itself. This is because mass-transfer limitations within the biofilm will be independent from the macroporous structure. Moreover, we previously observed that the cathodic biofilms in this system remained fairly thin (ca. 7.5 ± 2.5 μm in dry state).[13,14] At this small thickness, the diffusive mass transfer in the biofilm is very rapid, unlike some of the anodic biofilms that can become fairly thick, up to 100 μm,[28] and hence are potentially limited by mass transfer within the biofilm.

In comparison, different trends were observed in Figure 2A, which is more relevant when considering the reactor-engineering-application potential of each electrode material, as the performance is normalized to the projected surface area. For the same engineering evaluation purpose, similar trends were observed when normalizing performance to the electrode volume (Figure S2A). For the achievement of the maximal electrode performance, both the mass-transfer rate and the total surface area per unit volume are critical parameters from an overall productivity perspective. Therefore, the large porosity ("void space") and hence lower surface area for biofilm

DOI: 10.1021/acs.est.5b04431
Environ. Sci. Technol. 2016, 50, 1982−1989

development within the 10 ppi structure (2.54 mm average pore diameter; see Table S1) produced the lowest overall performance, with a current density of ca. −35 A m^{-2} and an acetate production rate of ca. 247 g m^{-2} day^{-1}. When the average pore diameter was decreased by a factor 4.5 (i.e., 0.56 mm; 45 ppi), the projected surface area performance was increased by a factor 2.9, achieving the highest MES rates with a current density of −102 A m^{-2} and an acetate production rate of 685 g m^{-2} day^{-1}. Similar current densities were achieved by Labele et al. (2014) in their MES systems, which, however, achieved lower product specificity with concomitant production of hydrogen and formate and only 40% electron recovery into acetate. Considering the 3D nature of EPD-3D, this corresponds to an acetate production rate of 66.5 kg $m_{electrode}^{-3}$ day^{-1} when normalized to electrode volume. The volumetric acetate production rate normalized to actual catholyte volume used in this study (250 mL) was obviously lower, around 0.37 g L^{-1} day^{-1} (see Figure S2B). However, the reactor configuration (e.g., electrode volume/catholyte volume ratio) was far from being optimized in this study. Nevertheless, this allows us to visualize the range of performance that could be achieved in an optimized system under the same conditions (e.g., same applied potential and pH) with the lowest rates when normalized to catholyte volume, while the rates normalized to electrode volume represents the maximal rates achievable. However, one can argue that substantial liquid volume is necessary to produce substantial amount of acetate. One should also not overlook the fact that true three-dimensional electrodes as used here with relatively large pores, which makes the intraporous liquid volume significant. Therefore, in continuous systems, other parameters such as the hydraulic retention time need to be considered and could allow approaching the highest production rates mentioned above. However, the total electrode surface area (electrode volume) to liquid volume ratio remains to be investigated but was out of the scope of this study. It can also be observed from Figure 2A that this strategy of increasing the total surface area per volume has its limit and that the associated reduction in mass-transfer rate can limit the overall productivity. A further decrease in pore size to 0.42 mm (60ppi) did achieve a slightly lower performance than for the 45 ppi electrodes, with −92 A m^{-2} current density and 620 g m^{-2} day^{-1} of acetate production. Therefore, for this reactor configurations and under the given forced mass-transfer conditions, an EPD-3D electrode pore diameter in the order of 0.6 mm is optimal.

Interestingly, this optimal pore size range in this setup is different to that found for anode biofilms[29] in similar reactor configurations. Although on a different electrode material and under stagnant conditions, in that work it was found that the optimal pore diameter was 2.2 mm (i.e., much larger than our finding). This difference could be due to the larger thickness of anodic biofilms. However, further investigations need to be carried out to determine the influence of different (forced) mass-transfer rates through the 3D electrode matrix. Indeed, this porosity influence is highly dependent on the actual flow rate through the electrode material. A better compromise between mass transfer and total surface area per volume unit available for biofilm development could then be found in a forced flow-through system, in which case the pore size could possibly be smaller to achieve the maximal performance.

Effect of Cathode Applied Potential. The effect of the applied cathode potential on the microbial electrosynthesis performance was investigated by linear-sweep voltammetry (LSV) on the 45 ppi electrode reactors in turnover condition (i.e., with a continuous gaseous CO_2 feed). In parallel, online flow monitoring of key target gases (H_2, CH_4, and CO_2) using the titration and off-gas analysis (TOGA) sensor was employed, as described in a previous study.[14] The TOGA measurements confirmed that no methane was produced during the course of the experiment (data not shown). The TOGA also allows to continuously monitor any H_2 that would be stripped off the reactor by the continuous gas flow (He-CO_2) bubbling through the reactor. The H_2 flow rate could then be determined, and the corresponding current transformed into H_2 as end-product was calculated (see the Materials and Methods section). H_2 that might have been produced but consumed within the biofilm, and hence is not detected by the TOGA sensor, is not taken into account by the parameter "current transformed into H_2".[14] Unlike long-term chronoamperometry tests, LSV experiments were too short to obtain an easily measurable change in acetate concentration during the potential scan. However, on the basis of the 100% electron conversion efficiency into acetate in continuous operating conditions at −0.85 V versus SHE applied cathode potential (see above) and building on previously reported results with the TOGA sensor, which proved that bioH_2-mediated electron-transfer mechanism operate these systems,[14] it is reasonable to assume that any current not recovered as H_2 flow during the LSV was converted into acetate. The total current consumed and the current converted into H_2 as well as the deducted acetate production along the potential range covered in the LSV are plotted in Figure 3. This experiment was run in duplicate, with the result being very similar, as shown in Figure S3. A comparison of biotic versus abiotic LSV can also be seen in Figure S4.

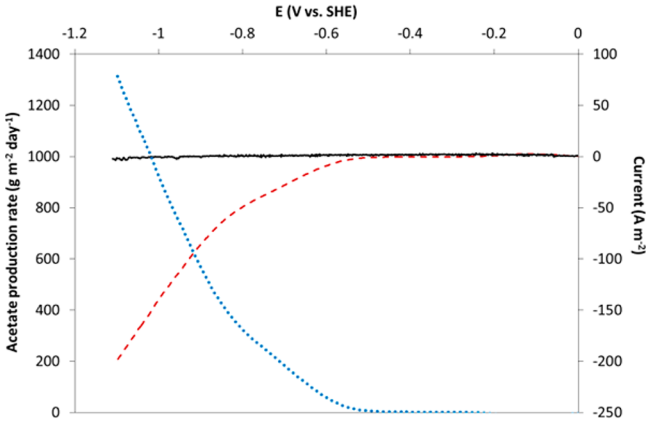

Figure 3. Linear-sweep voltammetry (current shown by dashed red line) of biotic reactor in turnover conditions recorded using the TOGA sensor. The solid (black) line represents the current converted into hydrogen, and the dotted blue line represents the calculated acetate production rate. The plotted values were normalized to projected surface area. Scan rate: 0.1 mV s^{-1}.

As previously reported, a clear shift of the reductive wave toward higher potential was observed compared to the abiotic control, which has been regarded as evidence of biological catalytic activity.[6,14,16,30] Acetate production started occurring at fairly high potential, ca. −0.5 V versus SHE. According to observations made during the chronoamperometry experiments described above, 100% of the electrons derived from the electrode were assimilated into acetate at −0.85 V versus SHE. However, more strikingly, 99% of the electrons were converted

DOI: 10.1021/acs.est.5b04431
Environ. Sci. Technol. 2016, 50, 1982−1989

into acetate at −1.1 V versus SHE, achieving a potential acetate production rate of 1330 g m^{-2} day^{-1} at this cathode potential. This corresponds to an impressive 130 kg m^{-3} day^{-1} of acetate, which means the above-reported production rate could be doubled by applying 250 mV lower cathode potential while still conserving very high product specificity. This observation could have an important impact for the practical application of this technology. It is very likely that the higher production rate would bring larger benefits in terms of capital cost savings (reducing the cathodic reactor volume) compared to the additional operating costs due to the higher power requirements to achieve the lower cathodic potential. Remarkably, a very high cathodic current density of about −200 A m^{-2} was reached at −1.1 V versus SHE. As previously reported, biologically induced hydrogen is the main electron shuttle from the electrode to the acetate-producing biomass, which forms a thin biofilm on the surface of the electrode.[14] This current density corresponds to a high hydrogen production rate (ca. 2.3 $m^3_{H_2}$ m^{-2} day^{-1}), and it highlights the very high hydrogen consumption capability of the acetogens located in the biofilm. It could be expected that such a high H_2 production rate would remove a biofilm from the electrode surface due to the large gas volume generated, although it corresponds to a smaller H_2 production of 85 L m^{-2} day^{-1} when normalized to total surface area. However, this experiment showed that the hydrogen-utilizing acetogens are able to cope very effectively with this hydrogen production. Furthermore, Figure 3 seems to indicate that −1.1 V versus SHE is most likely not the maximally applicable potential, and lower potentials could be applied to further increase the acetate production rate as long as the acetogenic biofilm can still fully convert the increased H_2 production. Such optimizations would need to be incorporated in an overall economic assessment to evaluate the impact of the higher power costs in relation to the maximum acetate production rate that can be achieved.

Effect of pH. Using the TOGA sensor, the effect of the operating pH on the MES performance of the 60 ppi EPD-3D was also assessed. Figure 4A shows the evolution of the total current consumed at an applied cathode potential of −0.85 V versus SHE (same as chronoamperometry tests above) as well as the current assimilated into H_2 as end-product, while the pH was decreased stepwise from 6.7 to 3. Figure 4B shows the electron recovery into H_2 and acetate production rate relative to the pH. No methane was detected by the TOGA sensor throughout this pH variation experiment.

Microbial electrosynthesis from CO_2 to acetate was found to be strongly dependent on the pH. Slight changes on the pH led to significant change on the total amount of electron consumed. Unlike the above chronoamperometry and LSV tests above, "only" about 97% of the electrons consumed were assimilated into acetate at pH 6.7. The most remarkable observation from this test is that an optimum pH of 5.2 was required to achieve the maximal acetate production rate of about 790 g m^{-2} day^{-1} (77 kg m^{-3} day^{-1}). From these results, we determined that the dominant soluble CO_2 form (HCO_3^- or H_2CO_3) did not seem to make any difference to the microbial activity. It has to be pointed out here that the 60 ppi electrode material was typically not achieving the best acetate production performance due to mass-transfer limitations in this configuration. This low operating pH is not only interesting because it achieves a 40% higher acetate production rate but also because it would likely inhibit any methanogenic activity. For large-scale

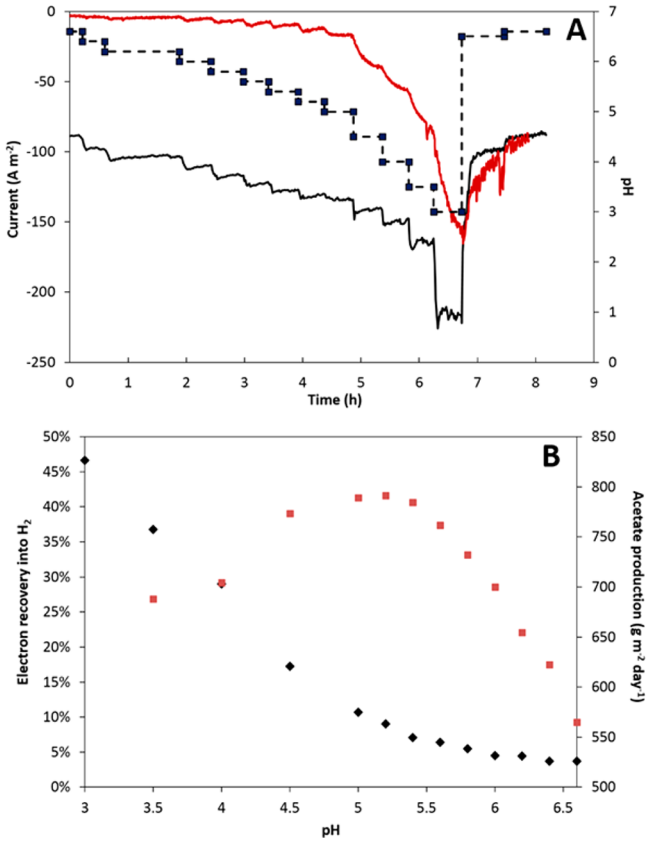

Figure 4. (A) pH variation experiment using the TOGA sensor. Both total current consumed (solid black line) and current converted into H_2 (solid red line) were followed at −0.85 V vs SHE applied cathode potential while the pH was decreased stepwise from 6.7 to 3 (black square, dashed line). The current values were normalized to projected surface area. (B) represents the electron recovery into H_2 (black diamond) and acetate production rate (red square) at each pH.

application, avoiding the addition of an external chemical inhibitor (bromoethanesulfonate) would have a large positive impact both technically and economically. This result confirms the findings of a recent study in which a continuous operation at a controlled pH of 5.8 achieved a higher acetate production rate than at higher pH.[11] It was not clear whether this was due to the direct effect of the low pH on the metabolism of the microorganisms or to the indirect increase of substrate availability. Because the main electron-transfer mechanism for acetate production has shown to be via biologically induced hydrogen,[14] the improved acetate production performance would likely be due to the direct effect of significantly higher proton availability at lower pH. This would further support the hypothesis that mass-transfer limitations into the 3D electrode matrix, likely in the form of limited proton availability, is the main reason for the reduced acetate production in the 60 ppi RVC foam compared to the more porous materials. Indeed, from all the reactants needed for acetate biolectrosynthesis, H^+ is by far the more diluted one in our reaction media, and, therefore, an increase of more than an order of magnitude in its concentration is very likely going to increase the production rate, provided that the microorganisms are still active at the new pH. The ongoing increase in current even below pH 5.2 demonstrates that even higher current densities can be achieved (at a given potential) by increasing the proton availability further. However, at these more acidic conditions, the

DOI: 10.1021/acs.est.5b04431
Environ. Sci. Technol. 2016, 50, 1982−1989

acetogenic activity seems to be limited, and hence, more current is converted to H_2 directly.

The effective inhibition of methane production would also have to be investigated in these conditions, without the bromoethanesulfonate addition, for a prolonged period of time. Moreover, we can observe in Figure 4B that about 9% of the electrons consumed were "lost" in H_2 and hence not assimilated into acetate, making the process slightly less specific. However, this could also be due to the fact that the culture was acclimated at pH 6.7 and that the duration of the pH variation steps was relatively short. It is believed that culture enrichment at a lower pH would remedy this.

Finally, it can be observed that pH lower than 4.5 is detrimental to the acetate-producing microorganisms. Significantly higher proportion of H_2 was detected. Remarkably, but in line with the previous electron-transfer-mechanism findings,[14] a significant absolute cathodic current increase was observed when the pH was decreased toward even lower pH, with the highest current density of about -220 A m^{-2} recorded at pH 3. We previously showed that hydrogen production was most likely due to the biological synthesis of copper particles, and the catalysis effect was maintained even after the biofilm was removed.[14] When the pH was increased back to 6.7, all the electrons were diverted to H_2 production only, confirming that pH that was too low removed or strongly inhibited the microorganisms. This finding has potential implication for pure H_2 large-scale implementation. Once the H_2 maximum performance is obtained due to biological activity, one can either decide to stop feeding CO_2 or sterilize the reactor to obtain H_2 as the sole product and could decrease the pH to low values to increase the production rate further. Taking into account the 3D nature of the electrode (2600 m^2 m^{-3}), a current of -220 A m^{-2} (22000 A m^{-3}) would correspond to ca. 250 $m^3_{H_2}$ m^{-3} day^{-1}, which is one of the highest H_2 production rates reported to date on MEC, to the best of our knowledge.

Use of Biogas as a Readily Available Carbon Dioxide Source. Another key consideration for potential practical applications is the source of carbon dioxide. Several options are available, but not all of them are attractive for MES applications to produce relatively low-value end-products such as acetate. Therefore, a cheap and readily available carbon dioxide source would be favored, which would likely be in a mixed gas situation. Biogas could be regarded as an interesting option in this context because it is primarily composed of methane (CH_4) and carbon dioxide. Biogas is produced during anaerobic digestion and can be used on-site for power generation but could also be more economically used as a transport fuel for buses, cars, etc. For the latter application, the CO_2 fraction needs to be removed to improve gas compression and storage and combustion efficiency. Therefore, an MES process to convert the CO_2 fraction to acetate could be perfectly suitable for such a biogas "cleaning" operation. This option could then be both environmentally and economically attractive for both applications (organics production and biogas utilization as fuel). Very recently, BES has also been proposed as a biogas upgrading technology with conversion of the CO_2 fraction to methane.[31]

Consequently, a synthetic biogas mixture, CH_4–CO_2 (70%:30% v/v), was fed to an MES reactor with 45 ppi EPD-3D electrode for a period of 2 weeks. The cathode potential was controlled at -0.85 V versus SHE and the pH at 6.7, while the current consumption and VFA production were followed over time. The current consumption evolution can be seen in Figure 5. A pair of chronoamperometry experiments in

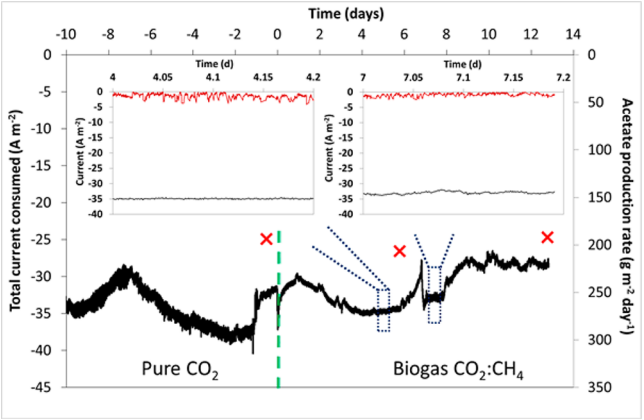

Figure 5. Current density evolution over time (solid black line) and acetate production rate (red cross) on EPD-3D 45 ppi while being fed with pure CO_2 from day -10 to day 0 and with a synthetic biogas mixture (CH_4–CO_2 70%:30% v/v) from day 0 onward at -0.85 V vs SHE applied cathode potential. The two inset graphs show the current converted into hydrogen (red solid line) measured on the TOGA during two distinct periods of the chronoamperometry test.

the same conditions were performed with the TOGA sensor, and the current converted into H_2 as the end-product in comparison to the total current consumed are shown in the insets in Figure 5.

We can observe that feeding the biogas mixture instead of pure CO_2 did not influence the total current consumed; the current had already decreased to about -30–35 A m^{-2} before this test, as observed in Figure 5. The chronoamperometry experiments run with the TOGA sensor also showed that no H_2 was detected from the reactor, and the VFA analyses over the 13 days of the experiment confirmed that 98 ± 2% of the electrons consumed were assimilated into acetate, with no other VFAs produced. Using biogas as carbon dioxide source showed, therefore, very similar MES performance as compared to using pure CO_2, making biogas a potentially useful and efficient CO_2 source for large-scale MES implementation. This test is mainly a successful proof of concept, and further investigations would need to be carried out using real biogas, which may also contain small traces of hydrogen sulfide that could affect MES performance.

■ ASSOCIATED CONTENT

Supporting Information

The Supporting Information is available free of charge on the ACS Publications website at DOI: 10.1021/acs.est.5b04431.

A table showing projected and total surface areas of each EPD-3D electrodes used in this study as well as their volumes and the average pore diameter of each RVC foam material. Additional details on calculations, electrochemical experiments, and off-gas and liquid analysis. A scheme showing the TOGA sensor experimental apparatus. Figures showing current density evolution over time on EPD-3D; maximum carbon dioxide consumption rate, acetate production rate, and cathodic current density; and linear sweep voltammetry of biotic reactor in turnover condition and both abiotic control and biotic reactor in turnover conditions. (PDF)

DOI: 10.1021/acs.est.5b04431
Environ. Sci. Technol. 2016, 50, 1982–1989

AUTHOR INFORMATION

Corresponding Author

*Phone: +31-(0)6-5396 6172; email: ludovic.jourdin@wur.nl.

Present Addresses

[§]Sub-Department of Environmental Technology, Wageningen University, Wageningen, The Netherlands.

[‖]Centro de Investigaciones y Transferencia-Jujuy-Conicet, Av. Bolivia 1239, San Salvador de Jujuy, 4600, Argentina.

Notes

The authors declare no competing financial interest.

ACKNOWLEDGMENTS

V.F. acknowledges a UQ Postdoctoral Fellowship. This work was supported by the Australian Research Council grant DP110100539. The authors also acknowledge Dr. J. Chen, Prof. G. Wallace, and the ARC Centre of Excellence for Electromaterials Science, University of Wollongong, NSW, Australia, for providing the EPD-3D electrodes.

REFERENCES

(1) Desloover, J.; Arends, J. B. A.; Hennebel, T.; Rabaey, K. Operational and technical considerations for microbial electrosynthesis. *Biochem. Soc. Trans.* **2012**, *40* (6), 1233−1238.

(2) Jourdin, L.; Freguia, S.; Donose, B. C.; Chen, J.; Wallace, G. G.; Keller, J.; Flexer, V. A novel carbon nanotube modified scaffold as an efficient biocathode material for improved microbial electrosynthesis. *J. Mater. Chem. A* **2014**, *2* (32), 13093−13102.

(3) Mikkelsen, M.; Jørgensen, M.; Krebs, F. C. The teraton challenge. A review of fixation and transformation of carbon dioxide. *Energy Environ. Sci.* **2010**, *3* (1), 43−81.

(4) Rabaey, K.; Girguis, P.; Nielsen, L. K. Metabolic and practical considerations on microbial electrosynthesis. *Curr. Opin. Biotechnol.* **2011**, *22* (3), 371−377.

(5) Lovley, D. R.; Nevin, K. P. Electrobiocommodities: powering microbial production of fuels and commodity chemicals from carbon dioxide with electricity. *Curr. Opin. Biotechnol.* **2013**, *24* (3), 385−390.

(6) Jourdin, L.; Freguia, S.; Donose, B. C.; Keller, J. Autotrophic hydrogen-producing biofilm growth sustained by a cathode as the sole electron and energy source. *Bioelectrochemistry* **2015**, *102* (0), 56−63.

(7) Rabaey, K.; Rozendal, R. A. Microbial electrosynthesis — revisiting the electrical route for microbial production. *Nat. Rev. Microbiol.* **2010**, *8* (10), 706−716.

(8) Lewis, N. S.; Nocera, D. G. Powering the Planet: Chemical Challenges in Solar Energy Utilization. *Proc. Natl. Acad. Sci. U. S. A.* **2006**, *103* (43), 15729−15735.

(9) Nevin, K. P.; Hensley, S. A.; Franks, A. E.; Summers, Z. M.; Ou, J.; Woodard, T. L.; Snoeyenbos-West, O. L.; Lovley, D. R. Electrosynthesis of organic compounds from carbon dioxide is catalyzed by a diversity of acetogenic microorganisms. *Appl. Environ. Microbiol.* **2011**, *77* (9), 2882−2886.

(10) Nevin, K. P.; Woodard, T. L.; Franks, A. E.; Summers, Z. M.; Lovley, D. R. Microbial electrosynthesis: Feeding microbes electricity to convert carbon dioxide and water to multicarbon extracellular organic compounds. *mBio* **2010**, *1* (2), 1−4.

(11) Batlle-Vilanova, P.; Puig, S.; Gonzalez-Olmos, R.; Balaguer, M. D.; Colprim, J. Continuous acetate production through microbial electrosynthesis from CO2 with microbial mixed culture. *J. Chem. Technol. Biotechnol.* **2015**, DOI: 10.1002/jctb.4657.

(12) Ganigue, R.; Puig, S.; Batlle-Vilanova, P.; Balaguer, M. D.; Colprim, J. Microbial electrosynthesis of butyrate from carbon dioxide. *Chem. Commun.* **2015**, *51* (15), 3235−3238.

(13) Jourdin, L.; Grieger, T.; Monetti, J.; Flexer, V.; Freguia, S.; Lu, Y.; Chen, J.; Romano, M.; Wallace, G. G.; Keller, J. High acetic acid production rate obtained by microbial electrosynthesis from carbon dioxide. *Environ. Sci. Technol.* **2015**, *49*, 13566.

(14) Jourdin, L.; Lu, Y.; Keller, J.; Flexer, V.; Freguia, S. Biologically-induced hydrogen production drives high rate/high efficiency microbial electrosynthesis of acetate from carbon dioxide. Submitted for publication, 2015.

(15) LaBelle, E. V.; Marshall, C. W.; Gilbert, J. A.; May, H. D. Influence of acidic pH on hydrogen and acetate production by an electrosynthetic microbiome. *PLoS One* **2014**, *9* (10), e109935.

(16) Marshall, C. W.; Ross, D. E.; Fichot, E. B.; Norman, R. S.; May, H. D. Electrosynthesis of Commodity Chemicals by an Autotrophic Microbial Community. *Appl. Environ. Microbiol.* **2012**, *78* (23), 8412−8420.

(17) Marshall, C. W.; Ross, D. E.; Fichot, E. B.; Norman, R. S.; May, H. D. Long-term operation of microbial electrosynthesis systems improves acetate production by autotrophic microbiomes. *Environ. Sci. Technol.* **2013**, *47* (11), 6023−6029.

(18) Min, S.; Jiang, Y.; Li, D. Production of acetate from carbon dioxide in bioelectrochemical systems based on autotrophic mixed culture. *J. Microbiol. Biotechnol.* **2013**, *23* (8), 1140−1146.

(19) Patil, S. A.; Arends, J. B. A.; Vanwonterghem, I.; van Meerbergen, J.; Guo, K.; Tyson, G. W.; Rabaey, K. Selective Enrichment Establishes a Stable Performing Community for Microbial Electrosynthesis of Acetate from CO2. *Environ. Sci. Technol.* **2015**, *49* (14), 8833−8843.

(20) Giddings, C. G. S.; Nevin, K.; Woodward, T.; Lovley, D. R.; Butler, C. S. Simplifying Microbial Electrosynthesis Reactor Design. *Front. Microbiol.* **2015**, *6*.10.3389/fmicb.2015.00468

(21) Agler, M. T.; Wrenn, B. A.; Zinder, S. H.; Angenent, L. T. Waste to bioproduct conversion with undefined mixed cultures: the carboxylate platform. *Trends Biotechnol.* **2011**, *29* (2), 70−78.

(22) Liu, C.; Gallagher, J. J.; Sakimoto, K. K.; Nichols, E. M.; Chang, C. J.; Chang, M. C. Y.; Yang, P. Nanowire−Bacteria Hybrids for Unassisted Solar Carbon Dioxide Fixation to Value-Added Chemicals. *Nano Lett.* **2015**, *15*, 3634−3639.

(23) Flexer, V.; Chen, J.; Donose, B. C.; Sherrell, P.; Wallace, G. G.; Keller, J. The nanostructure of three-dimensional scaffolds enhances the current density of microbial bioelectrochemical systems. *Energy Environ. Sci.* **2013**, *6* (4), 1291−1298.

(24) Flexer, V.; Marque, M.; Donose, B. C.; Virdis, B.; Keller, J. Plasma treatment of electrodes significantly enhances the development of anodic electrochemically active biofilms. *Electrochim. Acta* **2013**, *108* (0), 566−574.

(25) Gapes, D.; Keller, J. Analysis of biological wastewater treatment processes using multicomponent gas phase mass balancing. *Biotechnol. Bioeng.* **2001**, *76* (4), 361−375.

(26) Pratt, S.; Yuan, Z.; Gapes, D.; Dorigo, M.; Zeng, R. J.; Keller, J. Development of a novel titration and off-gas analysis (TOGA) sensor for study of biological processes in wastewater treatment systems. *Biotechnol. Bioeng.* **2003**, *81* (4), 482−495.

(27) Bechthold, I.; Bretz, K.; Kabasci, S.; Kopitzky, R.; Springer, A. Succinic acid: a new platform chemical for biobased polymers from renewable resources. *Chem. Eng. Technol.* **2008**, *31* (5), 647−654.

(28) Nevin, K. P.; Kim, B. C.; Glaven, R. H.; Johnson, J. P.; Woodard, T. L.; Methé, B. A.; Didonato, R. J., Jr; Covalla, S. F.; Franks, A. E.; Liu, A.; Lovley, D. R. Anode biofilm transcriptomics reveals outer surface components essential for high density current production in Geobacter sulfurreducens fuel cells. *PLoS One* **2009**, *4* (5), 1−11.

(29) Chen, S.; He, G.; Liu, Q.; Harnisch, F.; Zhou, Y.; Chen, Y.; Hanif, M.; Wang, S.; Peng, X.; Hou, H.; Schroder, U. Layered corrugated electrode macrostructures boost microbial bioelectrocatalysis. *Energy Environ. Sci.* **2012**, *5* (12), 9769−9772.

(30) Rozendal, R. A.; Jeremiasse, A. W.; Hamelers, H. V. M; Buisman, C. J. N. Hydrogen production with a microbial biocathode. *Environ. Sci. Technol.* **2008**, *42* (2), 629−634.

(31) Batlle-Vilanova, P.; Puig, S.; Gonzalez-Olmos, R.; Vilajeliu-Pons, A.; Balaguer, M. D.; Colprim, J. Deciphering the electron transfer mechanisms for biogas upgrading to biomethane within a mixed culture biocathode. *RSC Adv.* **2015**, *5* (64), 52243−52251.

DOI: 10.1021/acs.est.5b04431
Environ. Sci. Technol. 2016, 50, 1982−1989